Chapter 1

Theoretical and Experimental Overview

1.1 Deep Inelastic Scattering

To understand the structure of the nucleon it is useful to first introduce the original process which described the nucleon as having a sub-structure. This process is the Deep Inelastic Scattering (DIS) process where a lepton impinges on a nucleon denoted as

$$l(\ell) + N(P) \rightarrow l(\ell') + X(P_X),$$ (1.1)

where l denotes a lepton, N denotes a nucleon, X represents all products not detected and ℓ, ℓ', P and P_X are the four momentum for their respective lepton or nucleon. This process is an electromagnetic reaction where a the lepton is scattered via virtual photon exchange with the nucleon. The leading order Feynman diagram for this reaction is shown in Fig. 1.1.
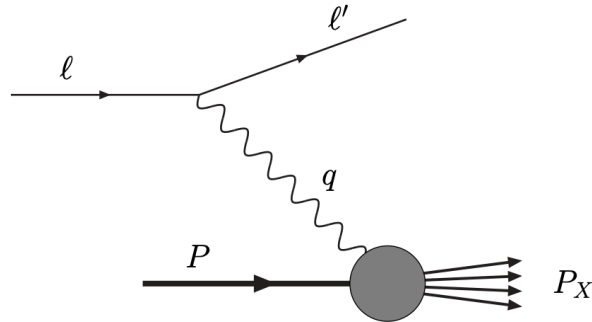

Figure 1.1: The leading order Feynman diagram for deep inelastic scattering

DIS is traditionally studied with a high energy lepton beam and a fixed nuclear target. The initial state kinematics are described by

$$s = (\ell + P)^2 \quad \text{or} \quad E,$$ (1.2)

where s is the center of mass energy and E is the energy of the lepton beam. The detected reaction kinematics in the lab frame are described by

$$Q^2 = -q^2 = -(\ell - \ell')^2 \approx EE'(1 - \cos\theta) \qquad (1.3)$$

$$x = \frac{Q^2}{2P \cdot q} = \frac{Q^2}{2M\nu} \qquad (1.4)$$

$$\nu = E - E' \qquad (1.5)$$

$$y = \frac{P \cdot q}{P \cdot \ell} = \frac{E - E'}{E} = \frac{\nu}{E} \qquad (1.6)$$

$$W^2 = (P + q)^2 \qquad (1.7)$$

where q is the virtual photon four momentum, E' is the scattered leptons energy, x is Bjorken x, ν is the change in energy of the scattered lepton, y is the inelasticity and W^2 is invariant mass of hadron final state. In the last relation from Eq. 1.3, θ is the scattering angle of the lepton with respect to the beam and the approximation is only true when the lepton mass is assumed to be zero. In Eq. 1.4, M is the nucleon mass. In the parton model, section 1.2, x has the interpretation as being the momentum fraction of the struck parton with respect to its parent hadron and therefore x ranges between 0 and 1. The inelasticity, y, measure the proportional lepton energy reduction and therefore takes on a value between 0 and 1.

The process is called deep if $Q^2 >> M^2$ and inelastic if $y < 1$. For practical purposes in experiments, the deep inelastic criteria corresponds to a $Q^2 > 1 \; GeV$ and $W^2 > M^2$. As can be seen in Eq. [1.3-1.7], not all the variables are independent. DIS is described by two independent variables usually given by (x, Q^2) or (x, y). For reference, in the limit as $y \to 1$ the process becomes elastic scattering and can then be described by only one independent variable.

The cross-section for DIS is defined as [8]

$$d\sigma = \frac{1}{4P \cdot \ell} \frac{e^4}{Q^4} L_{\mu\nu} W^{\mu\nu} 2\pi \frac{d^3\ell'}{(2\pi)^3 2E'} \qquad (1.8)$$

where $L_{\mu\nu}$ is the leptonic tensor and $W^{\mu\nu}$ is the hadronic tensor. The leptonic tensor describes free leptons and can therefore be calculated in perturbation theory. It can be decomposed into a systematic spin-independent tensor and an anti-symmetric spin-dependent tensor. Summing over all the possible spins of the lepton beam, the leptonic tensor is

$$L_{\mu\nu} = 2\left(\ell_\mu \ell'_\nu + \ell_\nu \ell'_\mu - g_{\mu\nu} \ell \cdot \ell'\right) + 2m\epsilon_{\mu\nu\rho\sigma} s^\rho q^\sigma \qquad (1.9)$$

where m is the lepton mass and s^ρ is the spin four vector of the lepton.

Generically the hadronic tensor is defined as

$$W^{\mu\nu} = \frac{1}{2\pi} \int \mathrm{d}^4\xi \, e^{iq\cdot\xi} \langle PS|J^\mu(\xi)J^\nu(0)|PS\rangle \tag{1.10}$$

where J is an electromagnetic current and $|PS\rangle$ represents the nucleon with momentum P and spin S. The hadronic tensor describes a hadron bound together by quantum chromo-dynamics (QCD). As of yet there is no known technique for calculating the hadronic tensor in a perturbation theory or otherwise. Instead the hadronic tensor can be written in the most general Lorentz invariant form using structure functions to parameterize the non-perturbative nature of the tensor. With the use of these structure functions, the differential DIS cross-section can be written

$$\frac{\mathrm{d}\sigma}{\mathrm{d}x\mathrm{d}y} = \frac{8\pi\alpha^2 ME}{Q^4}\left\{xy^2 F_1(x,Q^2) + \left(1-y\right)\frac{F_2(x,Q^2)}{x} + c_1(y,\frac{Q^2}{\nu})g_1(x,Q^2) + c_2(y,\frac{Q^2}{\nu})g_2(x,Q^2)\right\} \tag{1.11}$$

where α is the electromagnetic coupling constant; F_1, F_2, g_1, g_2 are structure functions; and c_1 and c_2 are functions which depend on the polarization of the target. The SLAC collaboration measured the structure functions, F_1 and F_2, and found mild variations as a function Q^2 [10, 12]. This phenomenon now known as Bjorken scaling lead to the theory of the parton model [9]. Fig. 1.2 shows the F_2 structure function which is approximately constant as a function of Q^2.

1.2   The Parton Model

The parton model is described in what is called an infinite momentum frame where the nucleon is moving which large momentum. In the parton model the nucleon, in high energy scattering processes, is considered to be composed of point like constituent mass-less particles called partons. At high energy scattering the QCD strong force binding the partons becomes asymptotic small and therefore the partons appear to be free. The cross-section in DIS can then be described as a lepton scattering incoherently off a free parton in the nucleon. In the parton model the hadron tensor for scattering off a quark can be written as [8]

$$W^{\mu\nu} = \frac{1}{2\pi}\sum_q e_q^2 \sum_X \int \frac{\mathrm{d}^3 P_X}{(2\pi)^3 2E_X} \int \frac{\mathrm{d}^4 k}{(2\pi)^4} \int \frac{\mathrm{d}^4 k'}{(2\pi)^4}\delta(k'^2)$$
$$\times [\bar{u}(k')\gamma^\mu\langle X|u(k)|PS\rangle] * [\bar{u}(k')\gamma^\nu\langle X|u(k)|PS\rangle] \times (2\pi)^4\delta^4(P-k-P_X)(2\pi)^4\delta^4(k+q-k'), \tag{1.12}$$

where e_q is the electric charge of quark flavor q; and u and $\bar{u}$ are free Dirac spinors. This hadronic tensor can be simplified by introducing the quark-quark correlation matrix as
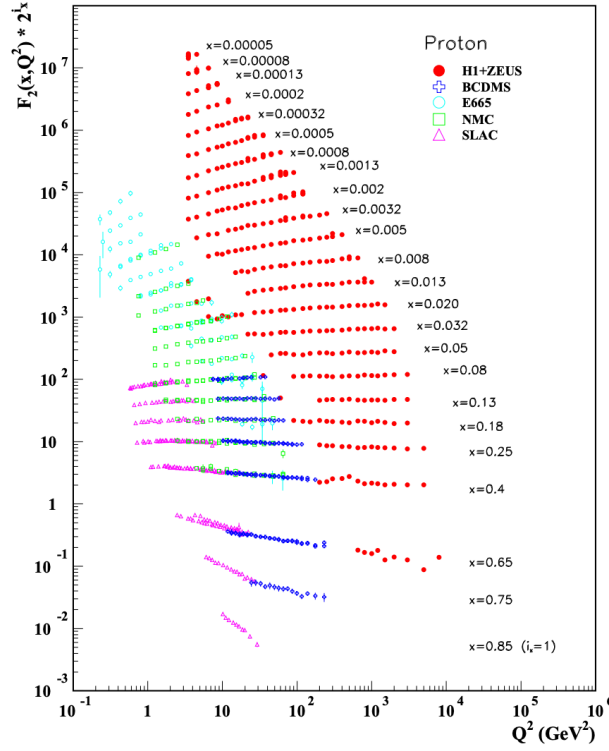
3

Figure 1.2: The F_2 structure function measured by several experiments. Note that the data is shifted up by a factor 2^{i_x} to see the x dependence. Image taken from [25]

$$\Theta_{ij}(k, P, S) = \sum_X \int \frac{\mathrm{d}^3 P_X}{(2\pi)^3 2E_X} (2\pi)^4 \delta^4(P - k - P_X) \times \langle PS|\phi_j(0)|X\rangle\langle X|\phi_i(0)|PS\rangle, \qquad (1.13)$$

where $\phi(\xi) = e^{-ip\cdot\xi}u(p)$ is a quark field. Using the quark-quark correlation matrix, the hadronic tensor can be written as

$$W^{\mu\nu} = \sum_q e_q^2 \int \frac{\mathrm{d}^4 k}{(2\pi)^4} \int \frac{\mathrm{d}^4 k'}{(2\pi)^4} \delta(k'^2)(2\pi)^4 \delta^4(k + q - k') \times \mathrm{Tr}[\Theta\gamma^\mu \slashed{k}'\gamma^\nu]. \qquad (1.14)$$

In the cases of unpolarized or longitudinally polarized DIS the lead order contributing terms from the quark-quark correlator are [7, 11, 21]

$$\Theta = \frac{1}{2}\Big(f_1(x)\slashed{P} + g_{1L}(x)\lambda\gamma_5\slashed{P} \Big) \qquad (1.15)$$

where λ is the longitudinal polarization of the hadron. The hadronic tensor simplifies to a symmetric contribution and an anti-symmetric contribution [8]

4

$$W_{\mu\nu}^{\text{symmetric}} = \frac{1}{P \cdot q} \sum_q e_q^2 \Big((k_\mu + q_\mu) P_\nu + (k_\nu + q_\nu) P_\mu - g_{\mu\nu} \Big) f_1^q(x), \qquad (1.16)$$

$$W_{\mu\nu}^{\text{anti-symmetric}} = \lambda \epsilon_{\mu\nu\rho\sigma} (k_\nu + q_\nu) P^\rho \sum_q e_q^2 g_{1L}^q(x), \qquad (1.17)$$

where in Eq. 1.15 f_1 and g_1 are two parton distribution functions (PDFs). f_1 is interpreted as the quark number density and g_{1L} is interpreted as the total quark helicity distribution in a hadron. f_1 is then refers to the density of unpolarized quarks in a hadron and g_{1L} refers to the density of quarks longitudinally polarized in the same longitudinal direction as the hadron. To make this explicit, f_1 and g_{1L} can be written

$$f_1 = f_1^+ + f_1^-, \qquad (1.18) \qquad\qquad g_{1L} = f_1^+ - f_1^-, \qquad (1.19)$$

where + and - denote the helicity. To be clear the parton distribution g_{1L} is not the same as the structure function g_1.

The unpolarized quark number density, f_1, has been extracted from global analysis of several experiments [17]. Fig. 1.3 shows the current xf_1 values and confidence intervals for different quarks and gluons specifically in the proton.
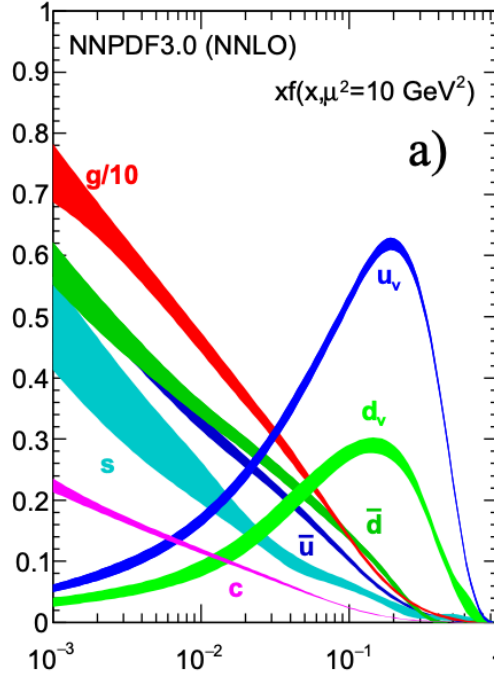

Figure 1.3: The unpolarized parton distribution functions times the momentum fraction. The different color correspond to different quarks or gluons. Image taken from [25]

The longitudinal spin structure, g_{1L} has also been measured at SMC, HERMES, and COMPASS [2, 4,

23]. The global analysis fit is shown in Fig. 1.4 using the parameterizations from NNPDF2014, AAC2008, DSSV2008 and LSS2010 [1, 18, 19, 22].
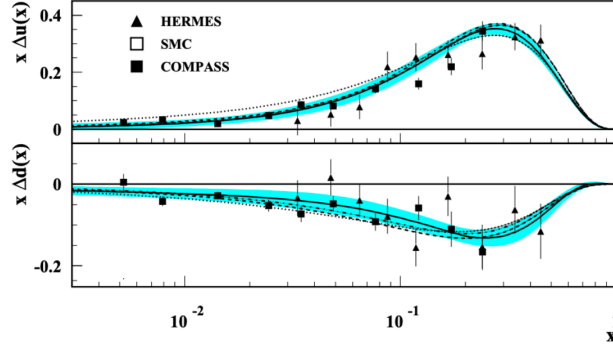

Figure 1.4: The longitudinally polarized parton distribution functions times the momentum fraction for the u-quark (top) and the d-quark (bottom). Image taken from [25]

In the parton model the structure function F_1 and F_2 are related to each other and to the unpolarized quark number as

$$F_2(x) = 2xF_1(x) = \sum_q e_q^2 x \left(f_1^q + f_1^{\bar{q}} \right) \tag{1.20}$$

which is known as the Callan-Gross relation [15]. As well the structure function g_1 is related to the helicity distribution, g_{1L}, as

$$g_1(x) = \frac{1}{2} \sum_q e_q^2 g_{1L}(x). \tag{1.21}$$

1.3 Transverse Momentum Dependence

The transverse momentum of the partons is integrated over when measuring the DIS process. This is because only the scattered lepton is measured and any transverse parton motion cannot be measured. The Drell-Yan process 1.5 and the SIDIS process 1.4 however are sensitive to the internal transverse momentum of the partons. In the limit of small transverse momentum compared to the virtual photon momentum and including the transverse parton momentum, the most generic leading order quark-quark correlator can be written [7, 11, 21]

$$\begin{aligned}
\Theta = \frac{1}{2} \Big[&f_1(x, k_\perp)\slashed{P} + \frac{1}{M} h_1^\perp(x, k_\perp)\sigma^{\mu\nu} k_\mu P_\nu + g_{1L}(x, k_\perp)\lambda\gamma_5\slashed{P} \\
&+ \frac{1}{M} g_{1T}(x, k_\perp)\gamma_5\slashed{P}(k_\perp \cdot S_\perp) + \frac{1}{M} h_{1L}^\perp(x, k_\perp)\lambda i\sigma_{\mu\nu}\gamma_5 P^\mu k_\perp^\nu + h_1(x, k_\perp)i\sigma_{\mu\nu}\gamma_5 P^\mu S_\perp^\nu \\
&+ \frac{1}{M^2} h_{1T}^\perp(x, k_\perp)i\sigma_{\mu\nu}\gamma_5 P^\mu \left(k_\perp \cdot S_\perp k_\perp^\nu - \frac{1}{2} k_\perp^2 S_\perp^\nu \right) + \frac{1}{M} f_{1T}^\perp(x, k_\perp)\epsilon^{\mu\nu\rho\sigma}\gamma_\mu P_\nu k_\rho S_\sigma \Big],
\end{aligned} \tag{1.22}$$

6

where $k_\perp$ denotes the transverse parton momentum and $S_\perp$ denotes the transverse hadron spin. Eq. 1.22 includes eight transverse momentum dependent (TMD) PDFs which are functions of x and $k_\perp$. The notation used to depict the TMDs functions is the so-called Amsterdam notation. The letters represent the different quark polarizations where f, g, h stand for unpolarized, longitudinally polarized and transversely polarized respectively. The subscript 1 denotes leading order and the subscripts T and L denote a transversely polarized hadron and a longitudinally polarized hadron respectively. Finally the superscript $\perp$ denotes that the distribution is an odd function of $k_\perp$ and therefore is zero when integrated over the parton transverse momentum. Fig. 1.5 organizes the TMDs by nucleon and quark polarizations and gives a visual of each TMD's interpretation.
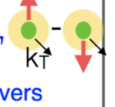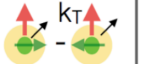

Figure 1.5: The eight TMDs needed to describe a spin $1/2$ nucleon at leading order. The columns represent the different nucleon polarization and the rows represent the different quark polarizations. The individual figures give a visual of the TMD's interpretation.

1.3.1 Sivers Distribution

The Sivers TMD was first purposed to explain large nucleon spin-dependent asymmetries [24]. The interpretation of the Sivers TMD, $f_{1,T}^{q\perp}(x, \mathbf{k_T})$, is that it gives a correlation between transverse spin of the parent hadron and transverse momentum of parton. When viewing the hadron in the direction of it's momentum, if $f_{1,T}^{q\perp}(x, \mathbf{k_T})$ is positive then it is expected that there are more partons with momentum going left than going right. Intuitively a non-zero $f_{1,T}^{q\perp}(x, \mathbf{k_T})$ would then imply that the bound quarks carry orbital angular momentum. As of yet however, there is no theoretical link between orbital angular momentum and the Sivers function.

The Sivers function is changes sign from naive time reversal. Naive time reversal is defined as reversing time but not swapping initial and final states [7]. The Sivers function is therefore said to be a T-odd function, and as a result it was originally believe to be a forbidden correlation. However it was shown that the Sivers function could be non-zero from gluon exchange during the initial state in the Drell-Yan process and during the final state in SIDIS [13,14]. Surprising it was shown that a non-zeron Sivers function is expected to have opposite sign in SIDIS and Drell-Yan [16]. That is

$$f_{1T}^{\perp}|_{Drell-Yan} = -f_{1T}^{\perp}|_{SIDIS}. \tag{1.23}$$

Include information on Bohr-Mulders, transversity and prezelosity (all TSAs determined in DY).

1.4 Semi-Inclusive Deep Inelastic Scattering

Semi-Inclusive Deep Inelastic Scattering (SIDIS) is the process where a lepton scatters electromagnetically off a nucleon and subsequently the scattered lepton and at least one scattered hadron are detected. As the name implies, SIDIS is related to the DIS reaction only SIDIS includes the addition of a detected hadron. SIDIS is denoted as

$$l(\ell, \lambda_l) + N(P, S) \rightarrow l(\ell') + h(P_h) + X(P_X), \tag{1.24}$$

where λ_l is the helicity of the incoming lepton, S is the spin of the nucleon, h is the detected hadron and P_h is the detected hadron's four momentum. The leading order one photon exchange Feynman diagram for the SIDIS process is shown in Fig. 1.6.
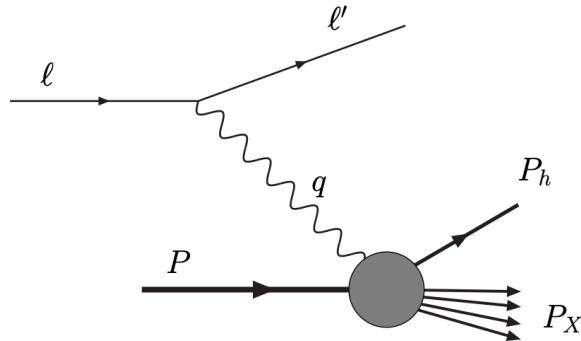

Figure 1.6: The semi-inclusive deep inelastic scattering leading order Feynman diagram

In addition to the kinematic variables used to describe DIS, Eq. [1.3-1.7], one more variable is needed to

describe the SIDIS process,

$$z = \frac{P \cdot P_h}{P \cdot q} \quad \overset{lab}{\underset{frame}{=}} \quad \frac{E_h}{E - E'},$$ (1.25)

which is interpreted as the fraction of possible energy the detected hadron can obtain. The transverse spin-dependent SIDIS cross-section can be described in a model independent way using structure functions as [7]

$$\frac{d\sigma}{dx\,dy\,d\psi\,dz\,d\phi_h\,dP_{h\perp}^2} = \frac{\alpha^2}{xyQ^2} \frac{y^2}{2\,(1-\varepsilon)} \left(1 + \frac{\gamma^2}{2x}\right) \left\{ F_{UU,T} + \varepsilon F_{UU,L} + \sqrt{2\,\varepsilon(1+\varepsilon)} \, \cos\phi_h \, F_{UU}^{\cos\phi_h} \right.$$

$$+ \varepsilon \cos(2\phi_h) \, F_{UU}^{\cos 2\phi_h} + \lambda_l \, \sqrt{2\,\varepsilon(1-\varepsilon)} \, \sin\phi_h \, F_{LU}^{\sin\phi_h}$$

$$+ |S_\perp| \left[\sin(\phi_h - \phi_S) \left(F_{UT,T}^{\sin(\phi_h-\phi_S)} + \varepsilon \, F_{UT,L}^{\sin(\phi_h-\phi_S)} \right) \right.$$

$$+ \varepsilon \, \sin(\phi_h + \phi_S) \, F_{UT}^{\sin(\phi_h+\phi_S)} + \varepsilon \, \sin(3\phi_h - \phi_S) \, F_{UT}^{\sin(3\phi_h-\phi_S)}$$

$$+ \sqrt{2\,\varepsilon(1+\varepsilon)} \, \sin\phi_S \, F_{UT}^{\sin\phi_S} + \sqrt{2\,\varepsilon(1+\varepsilon)} \, \sin(2\phi_h - \phi_S) \, F_{UT}^{\sin(2\phi_h-\phi_S)} \right]$$

$$+ |S_\perp|\lambda_l \left[\sqrt{1-\varepsilon^2} \, \cos(\phi_h - \phi_S) \, F_{LT}^{\cos(\phi_h-\phi_S)} + \sqrt{2\,\varepsilon(1-\varepsilon)} \, \cos\phi_S \, F_{LT}^{\cos\phi_S} \right.$$

$$\left. \left. + \sqrt{2\,\varepsilon(1-\varepsilon)} \, \cos(2\phi_h - \phi_S) \, F_{LT}^{\cos(2\phi_h-\phi_S)} \right] \right\},$$ (1.26)

where

$$\varepsilon = \frac{1 - y - \frac{1}{4}\gamma^2 y^2}{1 - y + \frac{1}{2}y^2 + \frac{1}{4}\gamma^2 y^2},$$ (1.27)

and $\gamma = \frac{2Mx}{Q}$ and ψ is the azimuthal scattering angle of the lepton around the lepton beam with respect to the transverse spin direction of the target. The SIDIS cross-section, Eq. 1.26, is defined in the γ-nucleon reference frame which is a target frame where the virtual photon is along the z-axis and the xz-plane is determined by the lepton plane. Fig. 1.7 shows the γ-nucleon lab frame and the relevant azimuthal angles.

The 14 structure functions in Eq. 1.26 are coefficients to the azimuthal angles. The structure functions are label as F where the superscript denotes which azimuthal angle coefficient they correspond to and the three subscripts represent the beam, target and virtual photon polarization from left to right respectively. The subscript polarizations are U for unpolarized, L for longitudinally polarized and T for transversely polarized. The cross-section, Eq. 1.26, is determined similarly to the DIS cross-section, Eq. 1.11, in that structure functions are used to generically parameterize the hadronic tensor.
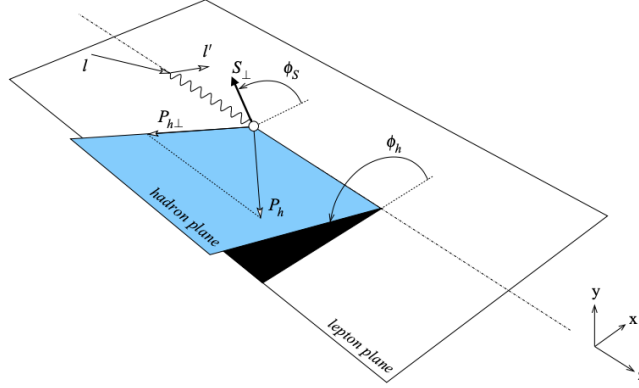
9

Figure 1.7: The γ-nucleon lab frame where the target nucleon is at rest and the virtual photon is along the z-axis. The lepton scattering plane defines the xz-plane where the outgoing lepton defines the positive x-direction. This image was taken from [7].

In the TMD regime the structure functions are related to TMD function and fragmentation functions (FF). That is to say where the detected hadron's transverse momentum is small compared to the virtual photon momentum, $P_{hT} << Q$, the model independent structure functions are related to TMD functions. The structure functions are equal to a convolution of a TMD and a FF in this regime where the convolution is defined as

$$\mathcal{C}[wfD] = x \sum_q e_q^2 \int d^2 p_T d^2 k_T \delta^{(2)}(p_T - k_T - P_{h\perp}/z) w(p_T, k_T) f^q(x, p_T^2) D^q(z, k_T^2), \qquad (1.28)$$

where w is a weight f is a TMD function and D is a FF. The relation between structure functions and TMDs at leading order for the structure functions related to transverse target polarization are [7]

$$F_{UT,T}^{\sin(\phi_h - \phi_S)} = \mathcal{C}\left[-\frac{\hat{h} \cdot p_T}{M} f_{1T}^\perp D_1\right] \qquad\qquad \propto f_{1T}^\perp \otimes D_1, \quad (1.29)$$

$$F_{UT,L}^{\sin(\phi_h - \phi_S)} = 0, \qquad\qquad (1.30)$$

$$F_{UT}^{\sin(\phi_h + \phi_S)} = \mathcal{C}\left[-\frac{\hat{h} \cdot k_T}{M_h} h_1 H_1^\perp\right] \qquad\qquad \propto h_1 \otimes H_1^\perp, \quad (1.31)$$

$$F_{UT}^{\sin(3\phi_h - \phi_S)} = \mathcal{C}\left[\frac{2(\hat{h} \cdot p_T)(p_T \cdot k_T) + p_T^2(\hat{h} \cdot k_T) - 4(\hat{h} \cdot p_T)^2(\hat{h} \cdot k_T)}{2M^2 M_h} h_{1T}^\perp H_1^\perp\right] \quad \propto h_{1T}^\perp \otimes H_1^\perp, \quad (1.32)$$

$$F_{LT}^{\cos(\phi_h - \phi_S)} = \mathcal{C}\left[\frac{\hat{h} \cdot p_T}{M} g_{1T} D_1\right] \qquad\qquad \propto g_{1T} \otimes D_1, \quad (1.33)$$

10

and the leading order structure functions related to an unpolarized target are

$$F_{UU,T} = \mathcal{C}[f_1 D_1] \qquad\qquad \propto f_1 \otimes D_1, \qquad\qquad (1.34)$$

$$F_{UU,L} = 0, \qquad\qquad (1.35)$$

where the unit vector $\hat{h} = P_{h\perp}/|P_{h\perp}|$ and D_1 and $H_1^\perp$ are fragmentation functions. The fragmentation functions are functions of z and describe the probability for a quark to hadronize to a specific hadron. These fragmentation functions depend on the quark spin, the hadron type and polarization and the quark k_T. In Eq. [1.29- 1.35] the fragmentation function D_1 refers to an unpolarized quark fragmenting to an unpolarized hadron and $H_1^\perp$ refers to a transversely polarized quark fragmenting to an unpolarized hadron.

The SIDIS cross-section, Eq. 1.26, can be rewritten in terms of asymmetries. These asymmetries are defined as

$$A_{BeamTarget}^{w_i(\phi_h,\phi_S)} = \frac{F_{BeamTarget}^{w_i(\phi_h,\phi_S)}}{F_{UU,T} + \varepsilon F_{UU,L}}, \qquad\qquad (1.36)$$

where $w_i(\phi_h, \phi_S)$ is the azimuthal angle associated with this asymmetry and $Beam$ and $Target$ represent the polarization of the beam and target. The asymmetry amplitude, Eq. 1.36, is a structure function divide by the unpolarized structure functions. This asymmetry amplitude definition is defined because it is easier to measure experimentally. In order to determine an asymmetry amplitude, the number of counts experimentally measures can be fit using a function in the form of Eq. 1.26 with the coefficients to each azimuthal amplitude as parameters to the fit. The result of the fit can determine the spin-dependent asymmetry amplitudes without needing to determine the luminosity.

COMPASS and HERMES measurements the asymmetry $A_{UT,T}^{\sin(\phi_h-\phi_S)}$ from the SIDIS reaction from a proton target [3,5]. The comparison of the result between these two collaboration is shown in Fig. 1.8. The asymmetry amplitude $A_{UT,T}^{\sin(\phi_h-\phi_S)}$ is related to the Sivers function and was measured to be non-zero at the level of 5%.

The top plots in Fig. 1.8 is the asymmetry for a positive detected hadron which is dominated by u-quark scattering and therefore by the u-quark Sivers function. This is the case for three reasons. Firstly because the SIDIS reaction is weighted by charge squared which therefore makes the u-quark scattering four times more likely. Secondly the so-called favor FF, where the detected hadron is the same charge as the which quark fragmented, is larger than the unfavored FF. Therefore a positively detected hadron most likely resulted from a positively fragmenting quark. Thirdly the proton target is composed twice as many u-quarks as
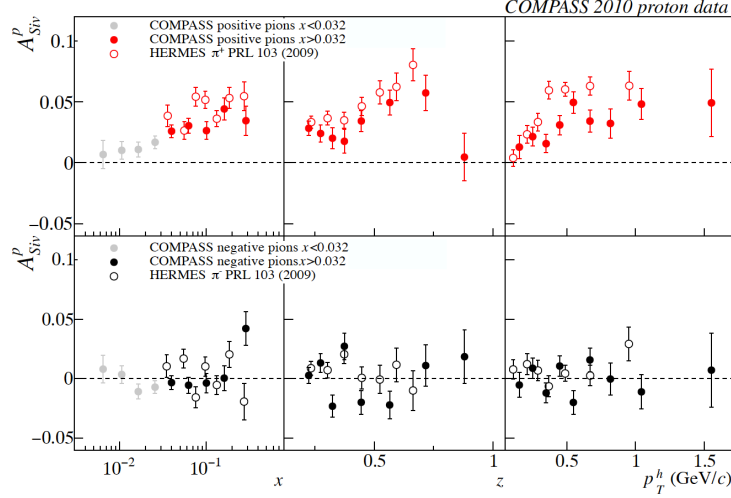
Figure 1.8: The asymmetry amplitude related to the Sivers function measure by COMPASS [5] and HER-MES [3]

d-quarks in this scattering kinematic region. For these three reasons the results in Fig. 1.8 imply that the u-quark Sivers function from the SIDIS reaction is positive.

The bottom plots in Fig. 1.8 suggest that the d-quark Sivers function in the SIDIS reaction is negative. The bottom results in Fig. 1.8 are from the combination of u-quark scattering then fragmenting unfavoredly and d-quark scattering and fragmenting favoredly. As was mentioned the charge weighting in the SIDIS reaction and the proton quark composition results in the u-quark scattering with a higher probability. On the other hand the favor FF for d-quark fragmenting to a negatively charged hadron versus the unfavored FF for u-quark fragmenting to a negatively charged hadron cancel the previous effect out. Therefore results in the bottom of Fig. 1.8 are for an equal combination from u-quark scattering and d-quark scattering. As the u-quark asymmetry amplitude is positive, the d-quark asymmetry amplitude must therefore be negative and so also must the d-quark Sivers function.

1.5   Drell-Yan

The Drell-Yan process is the reaction where a quark and an anti-quark annihilate and the end product results in two leptons. The Drell-Yan process is denoted as

$$H_a(P_a) + H_b(P_b, S) \rightarrow \gamma^* + X \rightarrow l(\ell) + l'(\ell') + X \tag{1.37}$$

where H_a and H_b are hadrons which carry the quark and anti-quarks and only the target hadron, H_b is considered to polarized with spin S. In this thesis the quark anti-quark pair annihilate to form a virtual

12

photon, γ^* and in addition the final state leptons detected are a muon and an anti-muon. The leading order one photon exchange diagram is shown in Fig. 1.9.
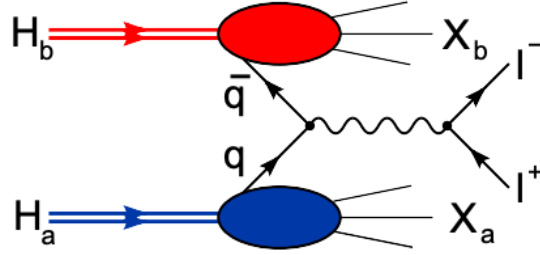

Figure 1.9: The Drell-Yan leading order diagram

The angles used to define the general Drell-Yan cross-section are defined with the use of two reference frames. The target frame (TF), Fig. 1.10a, defines the ϕ_S angle and the Collins-Soper (CS), Fig. 1.10b, frame defines the additional ϕ and θ angles. The ϕ_S angle is defined in TF as the angle between the transverse momentum of the virtual photon and the transverse spin of the target. The ϕ and θ angles, in the CS frame, are defined as the azimuthal and polar angle of the negatively charged muon.
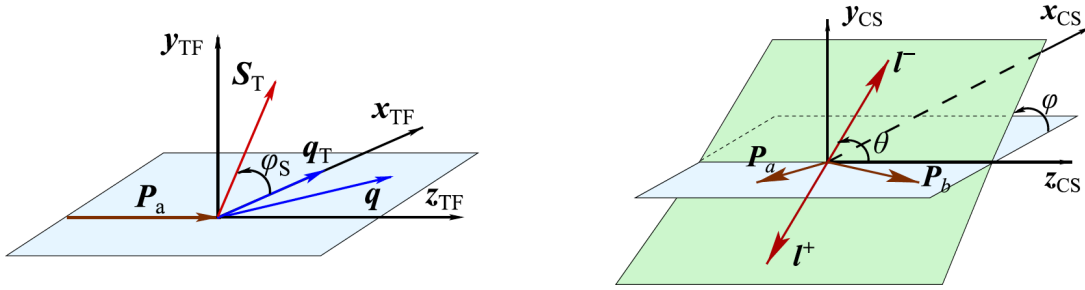
(a) The target frame where the z-axis is along the beam and the x-axis is in the direction of the transverse momentum of the virtual photon.

(b) The Collins-Soper frame is defined in the rest frame of the virtual photon where the z-axis bisects the beam and target momentum vectors.

The target frame is defined in the lab frame where the lab frame is rotated so the beam is along the z-axis and the transverse momentum of the virtual photon is along the x-axis. The y-axis in the target frame is then chosen so the coordinate system is right handed. The Collins-Soper frame is defined in the rest frame of the virtual photon where the xz-plane coincides with the hadron plane and the z-axis is chosen so it bisects the momentum vectors P_a and $-P_b$. The CS frame is defined from the target frame as a boost first along the along z-axis and then a boost along the x-axis so the rest frame of the virtual photon is reached. In this way the x-axis of the CS frame is defined and then the y-axis is again chosen so the coordinate system is

right handed.

The leading order model independent Drell-Yan differential cross-section for a polarized target is [6, 20]

$$
\begin{aligned}
\frac{d\sigma}{d^4q\, d\Omega} = \frac{\alpha_{em}^2}{F\, q^2} \Big\{ & \left((1+\cos^2\theta)\, F_U^1 + (1-\cos^2\theta)\, F_U^2 + \sin 2\theta \cos\phi\, F_U^{\cos\phi} + \sin^2\theta \cos 2\phi\, F_U^{\cos 2\phi} \right) \\
& + S_L \left(\sin 2\theta \sin\phi\, F_L^{\sin\phi} + \sin^2\theta \sin 2\phi\, F_L^{\sin 2\phi} \right) \\
& + |S_T| \Big[\left(F_T^{\sin\phi_S} + \cos^2\theta\, \tilde{F}_T^{\sin\phi_S} \right) \sin\phi_S + \left(F_T^{\sin(\phi+\phi_S)} \sin(\phi+\phi_S) + F_T^{(\sin\phi-\phi_S)} \sin(\phi-\phi_S) \right) \sin 2\theta \\
& + \left(F_T^{\sin(2\phi+\phi_S)} \sin(2\phi+\phi_S) + F_T^{\sin(2\phi-\phi_S)} \sin(2\phi-\phi_S) \right) \sin^2\theta \Big] \Big\},
\end{aligned}
\tag{1.38}
$$

where $F = 4\sqrt{(P_a \cdot P_b)^2 - M_a^2 M_b^2}$ is the flux and Ω is the solid angle of the outgoing negatively charged muon. The twelve model independent structure functions in Eq. 1.38 are labeled as $F_{Target\ polarization}^{azimuthal\ angle\ coefficient}$. The differential cross-seciton, Eq. 1.38, can be rewritten in terms of asymmetry amplitudes and depolarization factors. The asymmetry amplitudes are defined similarly to the case in SIDIS, Eq. 1.36, and again for the reason that asymmetries can be determined to a higher precision than structure functions. For Drell-Yan these asymmetry amplitudes are

$$
A_{Target}^{w_i(\phi,\phi_S)} = \frac{F_{Target}^{w_i(\phi,\phi_S)}}{F_U^1 + F_U^2}, .
\tag{1.39}
$$

The asymmetry amplitudes are the result of different virtual photon polarizations decaying to final state lepton pair. The depolarization factor is defined as the ratio of the virtual photon polarization to produce such an asymmetry to that of a transversely polarized virtual photon. The depolarization is defined for each asymmetry amplitude as

$$
D_{[f(\theta)]} = \frac{f(\theta)}{1 + A_U^1 \cos^2\theta},
\tag{1.40}
$$

where the function $f(\theta)$ is the virtual photon polarization responsible for the given asymmetry.

$$
\begin{aligned}
W_{\mu\nu} = & \left(\frac{q_\mu q_\nu}{q^2} - g_{\mu\nu} \right) \frac{F_1(x,Q^2)}{M} + \left(P_\mu - \frac{P\cdot q}{q^2} q_\mu \right) \left(P_\nu - \frac{P\cdot q}{q^2} q_\nu \right) \frac{F_2(x,Q^2)}{M^2\nu} \\
& + i\epsilon_{\mu\nu\rho\sigma} \frac{q^\rho}{P\cdot q} \left\{ S^\sigma g_1(x,Q^2) + \left(S^\sigma - \frac{S\cdot q}{P\cdot q} P^\sigma \right) g_2(x,Q^2) \right\},
\end{aligned}
\tag{1.41}
$$

where F_1, F_2, g_1 and g_2 are structure functions which are determined from experiments.

14

References

[1] I. Abt, A. M. Cooper-Sarkar, B. Foster, V. Myronenko, K. Wichmann, and M. Wing. Study of HERA ep data at low Q^2 and low x_{Bj} and the need for higher-twist corrections to standard perturbative QCD fits. *Phys. Rev.*, D94(3):034032, 2016.

[2] B. Adeva et al. The Spin dependent structure function g(1) (x) of the proton from polarized deep inelastic muon scattering. *Phys. Lett.*, B412:414–424, 1997.

[3] A. Airapetian et al. Observation of the Naive-T-odd Sivers Effect in Deep-Inelastic Scattering. *Phys. Rev. Lett.*, 103:152002, 2009.

[4] A. et al. Airapetian. Flavor decomposition of the sea-quark helicity distributions in the nucleon from semiinclusive deep inelastic scattering. *Phys. Rev. Lett.*, 92:012005, Jan 2004.

[5] M. Alekseev et al. Collins and Sivers asymmetries for pions and kaons in muon-deuteron DIS. *Phys. Lett.*, B673:127–135, 2009.

[6] S. Arnold, A. Metz, and M. Schlegel. Dilepton production from polarized hadron hadron collisions. *Phys. Rev.*, D79:034005, 2009.

[7] Alessandro Bacchetta, Markus Diehl, Klaus Goeke, Andreas Metz, Piet J. Mulders, and Marc Schlegel. Semi-inclusive deep inelastic scattering at small transverse momentum. *JHEP*, 02:093, 2007.

[8] Vincenzo Barone, Alessandro Drago, and Philip G. Ratcliffe. Transverse polarisation of quarks in hadrons. *Phys. Rept.*, 359:1–168, 2002.

[9] J. D. Bjorken and Emmanuel A. Paschos. Inelastic Electron Proton and gamma Proton Scattering, and the Structure of the Nucleon. *Phys. Rev.*, 185:1975–1982, 1969.

[10] Elliott D. Bloom et al. High-Energy Inelastic e p Scattering at 6-Degrees and 10-Degrees. *Phys. Rev. Lett.*, 23:930–934, 1969.

[11] Daniel Boer and P. J. Mulders. Time reversal odd distribution functions in leptoproduction. *Phys. Rev.*, D57:5780–5786, 1998.

[12] Martin Breidenbach, Jerome I. Friedman, Henry W. Kendall, Elliott D. Bloom, D. H. Coward, H. C. DeStaebler, J. Drees, Luke W. Mo, and Richard E. Taylor. Observed Behavior of Highly Inelastic electron-Proton Scattering. *Phys. Rev. Lett.*, 23:935–939, 1969.

[13] Stanley J. Brodsky, Dae Sung Hwang, and Ivan Schmidt. Final state interactions and single spin asymmetries in semiinclusive deep inelastic scattering. *Phys. Lett.*, B530:99–107, 2002.

[14] Stanley J. Brodsky, Dae Sung Hwang, and Ivan Schmidt. Initial state interactions and single spin asymmetries in Drell-Yan processes. *Nucl. Phys.*, B642:344–356, 2002.

[15] C. G. Callan and David J. Gross. High-energy electroproduction and the constitution of the electric current. *Phys. Rev. Lett.*, 22:156–159, Jan 1969.

[16] John C. Collins. Leading twist single transverse-spin asymmetries: Drell-Yan and deep inelastic scattering. *Phys. Lett.*, B536:43–48, 2002.

[17] Juan Rojo et. al. The PDF4lhc report on PDFs and LHC data: results from run i and preparation for run II. *Journal of Physics G: Nuclear and Particle Physics*, 42(10):103103, sep 2015.

[18] L. A. Harland-Lang, A. D. Martin, P. Motylinski, and R. S. Thorne. The impact of the final HERA combined data on PDFs obtained from a global fit. *Eur. Phys. J.*, C76(4):186, 2016.

[19] M. Hirai and S. Kumano. Determination of gluon polarization from deep inelastic scattering and collider data. *Nucl. Phys.*, B813:106–122, 2009.

[20] A. Kotzinian. Description of polarized π^- + N Drell-Yan processes.

[21] P. J. Mulders and R. D. Tangerman. The Complete tree level result up to order $1/Q$ for polarized deep inelastic leptoproduction. *Nucl. Phys.*, B461:197–237, 1996. [Erratum: Nucl. Phys.B484,538(1997)].

[22] Emanuele R. Nocera, Richard D. Ball, Stefano Forte, Giovanni Ridolfi, and Juan Rojo. A first unbiased global determination of polarized PDFs and their uncertainties. *Nucl. Phys.*, B887:276–308, 2014.

[23] I. A. Savin. COMPASS results on the nucleon spin structure. *Nucl. Phys. Proc. Suppl.*, 219-220:94–101, 2011.

[24] Dennis W. Sivers. Single Spin Production Asymmetries from the Hard Scattering of Point-Like Constituents. *Phys. Rev.*, D41:83, 1990.

[25] M. Tanabashi et al. Review of Particle Physics. *Phys. Rev.*, D98(3):030001, 2018.